PNAS
www.pnas.org

Supplementary Information for

Small molecule inhibits α-synuclein aggregation, disrupts amyloid fibrils and prevents degeneration of dopaminergic neurons

Jordi Pujols, Samuel Peña-Díaz, Diana F. Lázaro, Francesca Peccati, Francisca Pinheiro, Danilo González, Anita Carija, Susanna Navarro, María Conde-Giménez, Jesús García, Salvador Guardiola, Ernest Giralt, Xavier Salvatella, Javier Sancho, Mariona Sodupe, Tiago F. Outeiro, Esther Dalfó and Salvador Ventura

Salvador Ventura
Email: **Salvador.Ventura@uab.es**

This PDF file includes:

Supplementary Information Text
Figs. S1 to S10
Table S1
Captions for movies S1 to S2
References for SI reference citations

Other supplementary materials for this manuscript include the following:

Movies S1 to S2

www.pnas.org/cgi/doi/10.1073/pnas.1804198115

Supplementary Information Text

Materials and Methods

Protein Purification

cDNAs corresponding to WT α-Syn and A30P and H50Q mutants were cloned in a pET28(a) plasmid and transformed into an *E. coli BL21 DE3* strain. WT α-Syn and its variants were expressed and purified as described previously (1). Samples were lyophilised and kept at -80ºC until assayed.

Metabolic stability in human liver microsomes

SC-D at 0.1 μM final concentration was pre-incubated with pooled human liver microsomes in phosphate buffer (pH 7.4) for 5 min in a 37 ºC shaking water-bath (final microsomal protein concentration: 0.1 mg/mL) in duplicate. The reaction was initiated by adding NADPH-generating system and incubated for 0, 15, 30, 45, and 60 min. The reaction was stopped by transferring the incubation mixture to acetonitrile/methanol (1:1, v/v). Samples were then vortexed and centrifuged at 4 ºC. Supernatants were used for UPLC-MS/MS analysis on an SCIEX 5500 triple-quadrupole MS *(SCIEX, Framingham, Massachusetts, USA)*. Two reference compounds were tested in parallel: propranolol, which is relatively stable, and verapamil, which is readily metabolized in human liver microsomes.

In vitro aggregation of α-synuclein

Lyophilized α-Syn was dissolved in sterile PBS 1X to a final concentration of 210 μM and filtered through 22 μm membranes to remove α-Syn small protein aggregates. The aggregation reaction was carried out in a 96-well sealed plate. Each well contained 70 μM α-Syn (WT, A30P or H50Q), 40 μM Th-T in PBS 1X, a 1/8" diameter teflon polyball (*Polysciences Europe GmbH, Eppelheim, Germany*) and the absence or presence of compound at 100 μM in a total volume of 150 μL. The plate was fixed in an orbital culture shaker Max-Q 4000 (*ThermoScientific, Waltham, Massachusetts, USA*) and agitated at 100 rpm and 37ºC. Th-T fluorescence was measured every 2 h by exciting the samples through a 430–450 nm filter and collecting the emission signal with a 480–510 filter using a

Victor3.0 Multilabel Reader (*PerkinElmer, Waltham, Massachusetts, USA*). A minimum of three plate replicates were made for each condition and also measurement triplicates were taken for each time point. After compiling the fluoresce signals for each condition and measurement, means and standard error of mean (SEM) were used to fit the aggregation kinetics with equation (1),

$$\text{Equation (1)} \qquad \propto = 1 - \frac{1}{k_b\left(e^{k_a t}-1\right)+1}$$

where k_b and k_a indicate the homogeneous nucleation rate constant and the secondary rate constant, accounting for fibril elongation and secondary nucleation, respectively (2).

For the analysis of the disaggregation capacity of SC-D, 70 μM α-Syn was incubated as previously described for four days and the Th-T signal measured. Then, 3.75 μL of DMSO or SC-D 4 mM in DMSO were added to attain a 100 μM compound concentration in the assay. The plate was incubated for an additional 24 h and Th-T derived fluorescence signals were measured again.

Transmission Electron Microscopy (TEM)

α-Syn samples were diluted 1:10 in PBS 1X, sonicated for 5 minutes and 5 μL of the resulting mixture immediately placed on a carbon-coated copper grid. After 5 min, samples were carefully dried with a piece of filter paper to remove the excess of liquid and washed with MiliQ water twice. Then, 5 μL of a solution of 2% (w/v) uranyl acetate was placed on the top of the grid for 2 min. Uranyl acetate excess was removed with filter paper. Finally, grids were left to air-dry for 10 min. Images were obtained using a Transmission Electron Microscopy Jeol 1400 (*Peabody, Massachusetts, USA*) operating at an accelerating voltage of 120 kV. A minimum of 30 fields were screened for each sample to obtain representative images.

Light scattering

Total aggregate formation was measured by light scattering adding 120 μL of pre-aggregated α-Syn into a quartz cuvette. Samples were previously resuspended by carefully vortexing and pipetting and then excited at 300 and 340 to collect and 90° scattering

collected between 260 to 400 nm in a Cary Eclipse Fluorescence Spectrophotometer (*Agilent, Santa Clara, California, USA*).

Nanoparticle tracking analysis

End point α-Syn aggregation reactions were collected and diluted 1:100 with MiliQ water to a final volume of 1 mL. The sample was measured by using a Nanosight NS3000 (*Malvern Instruments Ltd, Malvern, United Kingdom*) recording the light scattering and trajectory of any particle in solution for 1 minute. All samples were measured in triplicate and analysed with NTA3.1 software (*Malvern Instruments Ltd, Malvern, United Kingdom*).

Protein Misfolding Cyclic Amplification (PMCA)

Lyophilised α-Syn was dissolved in Conversion Buffer (PBS 1X, 1% Triton X-100, 150 mM NaCl), supplemented with Complete Protease Inhibitor Mixture (*Roche Applied Science, Penzberg, Germany*), to a final concentration of 90 μM as previously described. Then, 60 μL of the α-Syn solution was placed in 200-μL PCR tubes containing 1.0 mm silica beads (*Biospec Products, Bartlesville, OK, USA*) and the mixture was subjected to 24-hour cycles of 30 s sonication and 30 min incubation at 37ºC, using a Misonix 4000 sonicator setted at 70% power. Every 24 h, 1 μL of PMCA-incubated sample was transferred to a fresh soluble α-Syn samples, repeated for 5 days. Treated samples were prepared by adding SC-D into 200-μL tubes to a final concentration of 128 μM, in order to maintain the 0.7:1 α-Syn:SC-D ratio used in original kinetic assays. Control samples were prepared with the corresponding concentration of DMSO (0.26%). All reactions were performed in triplicate.

After each cycle of PMCA, 10 μL of α-Syn aggregates were diluted to a final volume of 100 μL with PBS 1X and 40 μM Th-T. Th-T fluorescence was recorded by exciting at 445 nm and collecting the emission fluorescence between 460 to 600 nm in a Cary Eclipse Fluorescence Spectrophotometer (*Agilent, Santa Clara, California, USA*).

Proteinase K Digestion

18 µL of α-Syn aggregates coming from each cycle of PMCA were mixed with 6 µL of Proteinase K (5 µg/mL final concentration). After an incubation of 30 minutes at 37ºC, 8 µL of loading buffer containing 1% β-mercaptoethanol were added and the enzyme inactivated by an incubation for 10 min at 95ºC in a Thermocell Cooling&Heating Block (*BIOER, Hangzhou, Zhejiang Province, China*). Afterwards, 7 µL of each sample were loaded into a Tricine-SDS-PAGE gel together with unstained Protein Standard markers (*ThermoFisher Scientific, Waltham, Massachusetts, USA*). Gels were stained with Blue safe.

Nuclear Magnetic Resonance

WT ^{15}N-labeled α-Syn was expressed in *E. coli BL21 DE3* strain. Cells were previously grown in LB medium until an OD_{600} of 0.6 was reached. The cultures were centrifuged at 3000 rpm for 15 min and cells resuspended in minimal medium; 750 mL of miliQ water containing 100 µL $CaCl_2$ 1M, 2 mL $MgSO_4$ 2 M, 20 mL glucose 20%, 100 mL vitamins 100x (*Sigma-Aldrich, Darmstadt, Germany*), 200 mL salts M9 and 1 g $^{15}NH_4$ (*Cambridge Isotope Laboratories, Inc., Tewksbury, Massachusetts, USA*). After 1 h of incubation at 37ºC, protein expression was induced with 1 mM IPTG. Protein was purified as previously described (1).

^{1}H-^{15}N HSQC spectra were obtained at 20 ºC on a Bruker 600 MHz NMR spectrometer equipped with a cryoprobe in a sample containing 70 µM ^{15}N-labeled α-Syn, PBS buffer (pH 7.4), 2.5% d6-DMSO and 10% D_2O in the absence or in the presence of 100 µM SC-D.

Characterisation of SynuClean-D – Fibril interaction

α-synuclein fibril model

To predict the binding energy of SC-D on human α-Syn fibrils, a model composed of 10 strands was built based on PDB structure 2N0A (**Fig. S9A**) (3). The central part of the structure is characterized by parallel, in-register β-sheets with a greek-key topology, while the terminals are flexible loops. The full-length α-Syn strand comprises 140 residues; however, SC-D, with its planar aromatic structure, will interact with the ordered β portion of the fibril rather than with the unstructured flexible loops. For this reason, a reduced model of α-Syn fibril was constructed including only residues 34 to 99 of PDB 2N0A (**Fig. S9B**). This reduced model, whose validity as a model for the full fibril has been tested with molecular dynamics simulations, has been used in all calculations.

To justify the validity of this approximation, 10 ns molecular dynamics simulations were performed and the RMSD of the backbone was computed for residues 34 to 99 on both the full-length α-synuclein fibril model (**Fig. S9A**) and the reduced model (**Fig. S9B**). Additionally, for the reduced model, a 1 ns and a 100 ns simulations were performed, to assess the stability of the fibrillar structure as a function of the simulation time. Results are reported in **Fig. S10**, and indicate that along a 10 ns simulation the RMSD evolution is identical for the full and the reduced model, validating our approximation. As far as the stability of the fibril as a function of time is concerned, our simulations revealed that the model of α-synuclein fibril is only partially stable, as along the 100 ns simulation the high fluctuation of RMSD indicates that important structural deformations take place. This instability is likely due to the small size of the model, which only comprises 10 strands and is hardly representative, in terms of network of weak interactions, of a fully grown α-synuclein fibril. Within the 10 ns simulation, however, the RMSD fluctuation is lower. This observation determined the maximum time of production simulation, which was set to 3 ns just to avoid unphysical structural deformations.

Binding site prediction

To predict the interaction of SC-D with the model of α-Syn fibril we used the Protein Energy Landscape Exploration (PELE) methodology (4, 5). PELE combines a Monte Carlo stochastic approach with protein structure prediction algorithms, and is able, among several options, to predict the binding poses of a small ligand on a protein without any beforehand crystallographic information. The general workflow of PELE is composed of three steps: i) a localized perturbation (random translation and rotation of the ligand, but it may also involve the backbone of the protein); ii) a side chain sampling based on a rotamer library; iii) a minimization, involving the full system. The OPLS2005 force field is employed and solvation effects are accounted for with the Generalized Born method (6, 7). Owing to the stochastic nature of PELE, several independents runs need to be performed on the same protein-ligand pair to ensure a full exploration of the conformational space. We ran 150 independent trajectories for the α-Syn/compound pair, providing a satisfactory sampling.

Molecular dynamics simulations indicate that despite the fact that SC-D is fully inserted between the parallel β-sheets, it is still in contact with water molecules along the whole simulation. This is not surprising owing to the wealth of polar group that are attached to the aromatic ring, and again corroborates the hypothesis that the main interaction of SC-D with the fibril is of van der Waals type. These interactions are represented as green patches (**Fig. S6**).

Binding energy calculation

We evaluated the binding energy of the poses predicted by PELE with the MM/GBSA method as implemented in the Amber16 suite (8, 9). In the MM/GBSA method, the binding energy is estimated based on a collection of frames, which were generated with molecular dynamics simulations run with the ff14SB force field, with the ligand topology generated using the General Amber Force Field and atomic partial charges fitted on the electrostatic potential computed at the B3LYP/6-31+G(d,p) level of theory with the Gaussian 09 package (10, 11). The PELE structures are neutralized with the appropriate number of counterions (Na^+/Cl^-) and water molecules are added up to a minimum distance of 8 Å

from the protein. The protocol for the molecular dynamics simulations is as follows: i) 2000 steps of minimization; ii) a 200 ps equilibration run in the NVT ensemble rising the temperature from 0 to 100 K, with a 4.0 kcal mol^{-1} constraint on the backbone, to avoid strong deformations; iii) a 2 ns run in the NPT ensemble, with the temperature rising from 100 to 300 K in the first half, and kept constant to 300 K in the second half, with a 2.0 kcal mol^{-1} constraint on the backbone, again to avoid strong deformations; iv) 5 independent 3 ns production runs in the NPT ensemble with the temperature kept constant to 300 K, with no constraints. A Langevin thermostat and a Monte Carlo barostat were employed. 20 geometries were evenly sampled from the last 2 ns of each trajectory of the production run, and the resulting 100 structures were used for binding free energy calculations neglecting the entropy term. The free energy values were computed on the ligand/fibril complex trajectory. An ionic strength of 100 mM, which is compatible with that of a biological buffer, was employed, and the igb5 generalized Born model of Amber16 was used. In this model, the Born radii are re-scaled to obtain a better agreement with the electrostatic component of solvation energy calculated by the Poisson-Boltzmann treatment in proteins (12).

Non-covalent interactions prediction

Non-covalent interactions were studied with the NCIPLOT program according to the methodology proposed by Yang and co-workers (13). The reduced density gradient s(r) (Eq. 2) is plotted against the electron density ρ multiplied by the sign of the second eigenvalue of the density Hessian. Peaks in the negative region of the x-axis in **Fig. 3C** are indicative of attractive interactions, while peaks in the positive regions are indicative of repulsive (non-bonded) contacts.

Equation (2) $$s(\boldsymbol{r}) = \frac{1}{2(3\pi^2)^{1/3}} \frac{|\nabla\rho|}{\rho^{4/3}}$$

Cytotoxicity assay

For human neuroglioma cells (H4), 40,000 cells were plated in a 24-well plate. After 24h, cells were treated with different concentrations of the compound or with vehicle (DMSO). Cells were the fixed after 24h with 4% PFA for 10 min, permeabilized with 0,1% triton X-

100 for 20 min, and stained with DAPI (1:5000) for 10 min. With the Olympus IX81-ZDC microscope system, 36 fields were randomly taken with 10x objective, in 6 independent experiments. The number of cells was counted using the Olympus Scan^R Image Analysis Software and the results analyzed using Graphpad Prism software (GraphPad Software, La Jolla, California, USA).

For human neuroblastoma cells (SH-SY5Y), 4000 cells/well were seeded into 96 well-plates and cultured in DMEM medium supplemented with 10% FBS. Then, SC-D was added at a range from 10 μM to 1 mM into each well. Treated and untreated cells were incubated at 37 ºC for 72 h. Then, 10 μL of PrestoBlue® reagent (*ThermoFisher Scientific, Waltham, Massachusetts, USA*) was added and, after an incubation for 10 minutes at 37 ºC, the fluorescence emission was recorded at 590 nm by exciting at 560 nm.

In-cell aggregation of endogenous α-synuclein

Cell Culture

Human neuroglioma cells (H4) were maintained in Opti-MEM I Reduced Serum Medium (*Life Technologies-Gibco, Thermo Fisher Scientific, Waltham, Massachusetts, USA*) supplemented with 10% fetal bovine serum Gold (FBS) (*PAA, Cölbe, Germany*) and 1% Penicillin-Streptomycin (*PAN, Aidenbach, Germany*). Cells were grown at 37 °C with 5% of CO_2 atmosphere.

Cell Transfection

Twenty-four hours prior to transfection, H4 cells were plated in 12-well plates (*Costar, Corning, New York*). The cells were transiently transfected according to the calcium phosphate method. Equal amounts of plasmids encoding a C-terminally modified α-Syn (SynT construct) were diluted in H_20 and 2.5 M $CaCl_2$. The mixture was then added dropwise and vigorously mixed into 2xBES-buffered saline solution containing phosphate ions (50 mM BES, 280 mM NaCl, 1.5 mM $Na_2HPO_4xH_2O$, pH 6.98). Fresh media was added to the cells during the 20 min of incubation. 16 h after transfection, cells were treated with different concentrations of the compound (1 or 10 μM). DMSO was used as the

vehicle. Finally, at 24 h the cells were fixed and subjected to immunocytochemistry to examine α-Syn inclusions formation.

Immunocytochemistry

After the treatment, cells were fixed with 4% paraformaldehyde for 10 min at room temperature followed by 20 min of permeabilization with 0.1% Triton X-100 (*Sigma-Aldrich, Darmstadt, Germany*) at room temperature. The cells were blocked in 1.5% normal goat serum (PAA)/PBS for 1 h, and then incubated for 3 h with mouse anti-α-Syn primary antibody (1:1000, *BD Transduction Laboratories, USA*). Afterwards, cells were washed three times with PBS and incubated with a secondary antibody (Alexa Fluor 488 donkey anti-mouse IgG) for 2 h at room temperature. Finally, cells were stained with Hoechst 33258 (*Life Technologies- Invitrogen, Carlsbad, California, USA*) (1:5000 in PBS) for 5 min and maintained in PBS for epifluorescence microscopy.

Quantification of α-synuclein inclusions

Quantifications were performed as previously described (14). Briefly, transfected cells were detected and scored based on the α-Syn inclusions pattern. Results were expressed as the percentage of the total number of transfected cells. At least 50-100 cells were counted *per* condition.

Caenorhabditis elegans models of PD

Media

Nematodes were cultured and maintained following standard procedures (17). Briefly, animals were synchronized by hypochlorite bleaching, hatched overnight in M9 buffer (3 g/L KH_2PO_4, 6 g/L Na_2HPO_4, 5 g/L NaCl, 1 M $MgSO_4$), and subsequently cultured at 20 °C on nematode growth medium (NGM) [1 mM $CaCl_2$, 1 mM $MgSO_4$, 5 μg/mL cholesterol, 250 M KH_2PO_4 (pH 6.0), 17 g/L Agar, 3 g/L NaCl] plates seeded with the *E coli* OP50 strain (OD600 values between 1.3-1.6).

C. elegans strains

NL5901, *unc-119(ed3)* III; *pkIs2386 [Punc-54::α-SYN::YFP; unc-119(+)*] and N2 (*Bristol*) wild type strains were obtained from the *Caenorhabditis elegans Genetic Center* (CGC). To analyse α-Syn induced dopaminergic degeneration, we used the strain UA196 (15), gifted generously by the laboratory of Dr Guy Caldwell (*Department of Biological Science, The University of Alabama, Tuscaloosa, USA*), (*sid-1(pk3321)*; *baIn33* [*Pdat-1::sid-1*, *Pmyo-2::mCherry*]; *baIn11* [*Pdat-1::α-SYN; Pdat-1::GFP*]). This strain was named *Pdat-1::GFP; Pdat-1::α-SYN* in the main text.

SynuClean-D administration

SynuClean-D was administered within NGM agar media and within the food source E. coli *OP50* strain. Briefly, 100 μM of a stock SC-D in 0.2% Dimethyl sulfoxide (DMSO) was added to liquid warm NGM to a final concentration of 10 μM. 250 μL of the *E. coli OP50* strain, containing 10 μM of SC-D or 0.2% of DMSO as control were added to dried plates, allowing the liquid to soak into the plates. Seeded plates were dried 24 hours before transferring the worms. Worms were transferred onto SC-D-seeded plates directly at larval stage L4, exposed to SC-D for 7 days and transferred daily to avoid cross progeny. EGCG was administered in the same manner.

Aggregate quantification

The quantification of aggregates was performed as previously described (16, 17). Briefly, NL5901 *pkIs2386* [*Punc-54::α-SYN::YFP; unc-119(+)*] animals were age-synchronized and left overnight to hatch. L1 animals were grown onto individual NGM plates containing *E. coli* OP50 to reach L4 developmental stage. Afterwards, L4 animals were transferred onto SC-D containing plates, while NGM plates containing only DMSO were used as negative control. Worms were transferred daily to avoid cross contamination. Aggregates were counted for each animal staged at L4+7 days in the posterior part. For each independent experiment, thirty 7-days old worms of each treatment were examined under a Nikon Eclipse E800 epifluorescence microscope equipped with an Endow GFP HYQ

filter cube (*Chroma Technology Corp, Bellows Falls, Vermont USA*) and each experiment was performed by triplicate. Aggregates were defined as discrete, bright structures, with boundaries distinguishable from surrounding fluorescence. Measurements of the inclusions were performed using ImageJ software considering the area dimensions.

Thrashing assays

Animals from the strain NL5901 [*unc-119(ed3)* III; *pkIs2386* [*Punc-54::α-Syn::YFP*; *unc-119(+)*] (SC-D treated and non-treated) at L4+7 days of development, were placed individually in a drop of M9 buffer and allowed to recover for 120 s (to avoid observing behaviour associated with stress). Afterwards, the number of body bends was recorded for 1 min. Non-treated N2 wild type animals were used as control. Movies of swimming worms were recorded using a Leica MZFFLIII stereomicroscope at nominal magnification of 30X and the Hamamatsu ORCA-Flash 4.0LT camera at 17 frames per second (17 fps) for 1 min. Bends per minute were obtained with the Worm Tracker pluggin (wrMTrck), from the ImageJ software. Thirty animals were counted in each experiment unless stated otherwise. Experiments were carried out in triplicate. Statistical analysis was performed using Graphpad Prism software (*GraphPad Software, La Jolla, California, USA*).

Blinding of experiments and replicates

Thrashing, or body bending studies were completed such that the experimenter was blind to the genotype of the worms. Strains were given letter codes by another member of the laboratory and the code was not broken until all of the replicates for a particular assay were completed. For all assays, we completed a minimum of three biological replicates per strain.

C. elegans neurodegeneration assays

Worms were analyzed for α-Syn -induced dopaminergic neurodegeneration as described previously (17). Briefly, 20-30 L4 staged animals from the strain UA196 were transferred to SC-D-NGM plates and were grown for seven days after which the dopaminergic cell death induced by the over-expression of α-Syn was analysed by fluorescence. Plates

containing only 0.2% DMSO, without SC-D, were used as control. Worms were transferred daily to avoid cross contamination.

The six anterior DA neurons (four CEP and two ADE DA neurons) were scored for neurodegeneration according to previously described criteria (18). Worms were considered normal when all six anterior DA neurons (four CEP (cephalic) and two ADE (anterior deirid) were present without any visible signs of degeneration. If a worm displayed degeneration in at least one of the six neurons, it was scored as exhibiting degeneration. For each independent experiment, thirty worms of each treatment were examined under a Nikon Eclipse E800 epifluorescence microscope equipped with an Endow GFP HYQ filter cube (*Chroma Technology Corp, Bellows Falls, Vermont, USA*).

Microscopy and imaging

Animals were placed in a 1 mM solution of sodium azide and mounted with a coverslip on a 4% agarose pad. Animals were visualized with a Nikon Eclipse E800 epifluorescence microscope. The system acquires a series of frames at specific Z-axis position (focal plane) using a Z-axis motor device. Animals were examined at 100× magnification to examine α-Syn induced DA cell death and at 40X to examine α-Syn apparent aggregates.

Statistical analysis

All graphs were generated with GraphPad Prism 6.0 software (*GraphPad Software Inc, La Jolla, California, USA*). Data were analysed by two-way ANOVA Tukey test using SPSS software version 20.0 (*IBM Analytics, Armonk, NY, United States*). All data are shown as means and standard error of mean (SEM). $p < 0.05$ was considered statistically significant. In the graphs *, ** and *** indicate $p < 0.05$, $p < 0.01$ and $p < 0.001$, respectively.

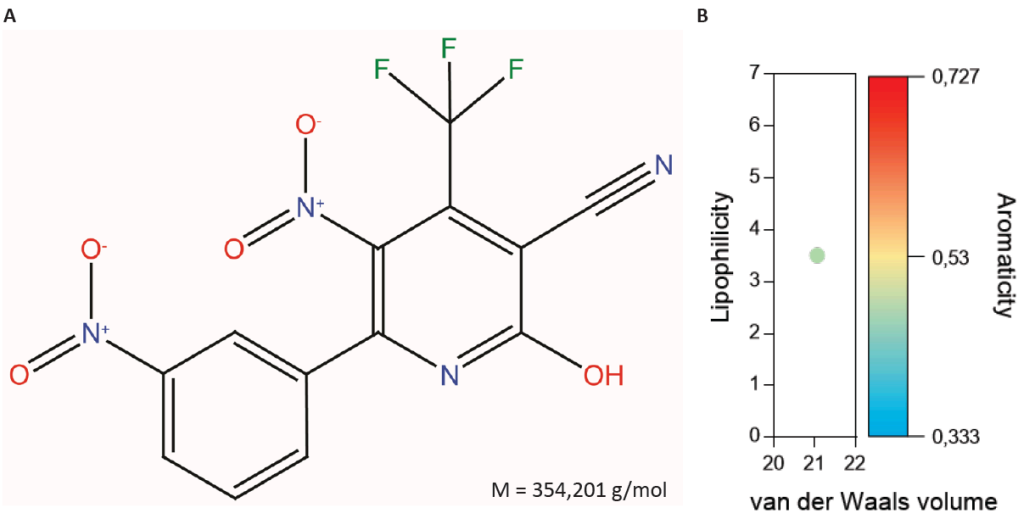

Figure S1. 2-hydroxy-5-nitro-6-(3-nitrophenyl)-4-(trifluoromethyl)nicotinonitrile or SynuClean-D (SC-D). Chemical structure (A) and properties (B) of the compound. Lipophilicity is defined as the Ghose–Crippen octanol/water coefficient (22). The volume corresponds to the sum of atomic van der Waals volumes (23). Aromaticity is defined as the ratio of the number of aromatic atoms to the total number of atoms.

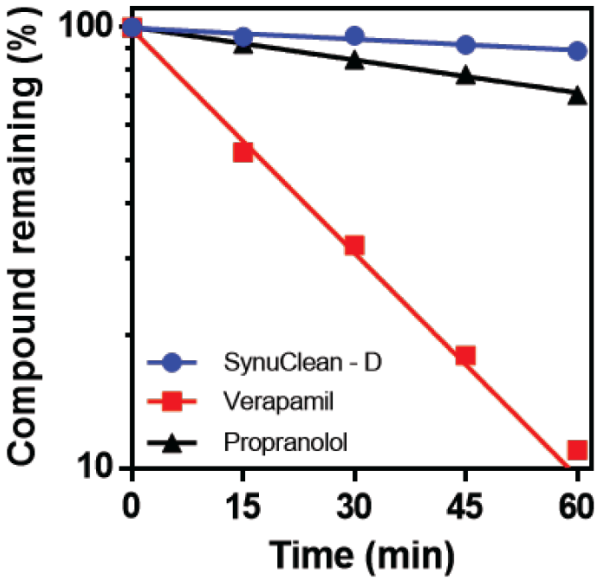

Figure S2. Metabolic stability of SC-D in human liver microsomes. The percentage of remaining compounds is plotted as a function of the incubation time at 37 ºC. Propranolol and verapamil are slowly and rapidly metabolized reference compounds, respectively. The data correspond to the mean of two experiments. The calculated $T_{1/2}$ of SC-D, propranolol and verapamil are 357.2, 119.5 and 19.0 min, respectively. The calculated intrinsic clearance values for SC-D, propranolol and verapamil are 3.9, 11.6 and 73.1 µL/min/mg, respectively.

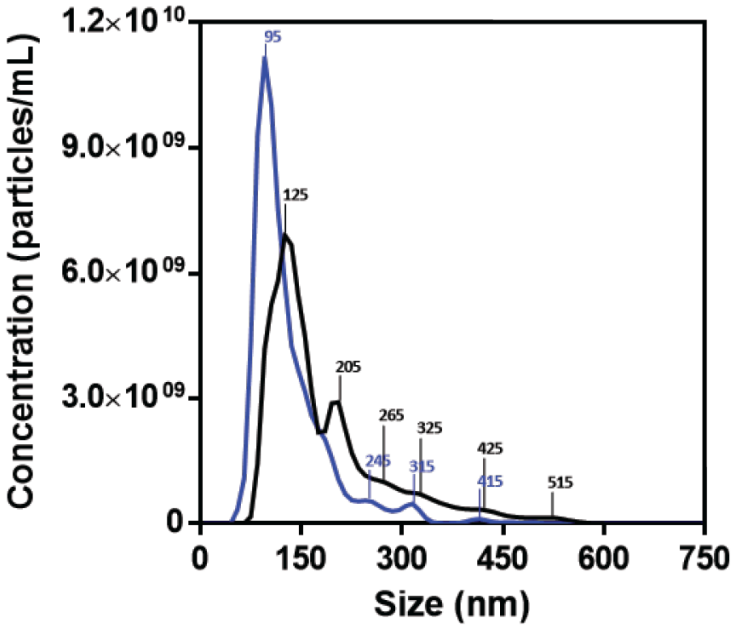

Figure S3. Fibril size characterization. Determination of the different fibril size population in absence (black) and presence (blue) of SC-D by using nanosight system.

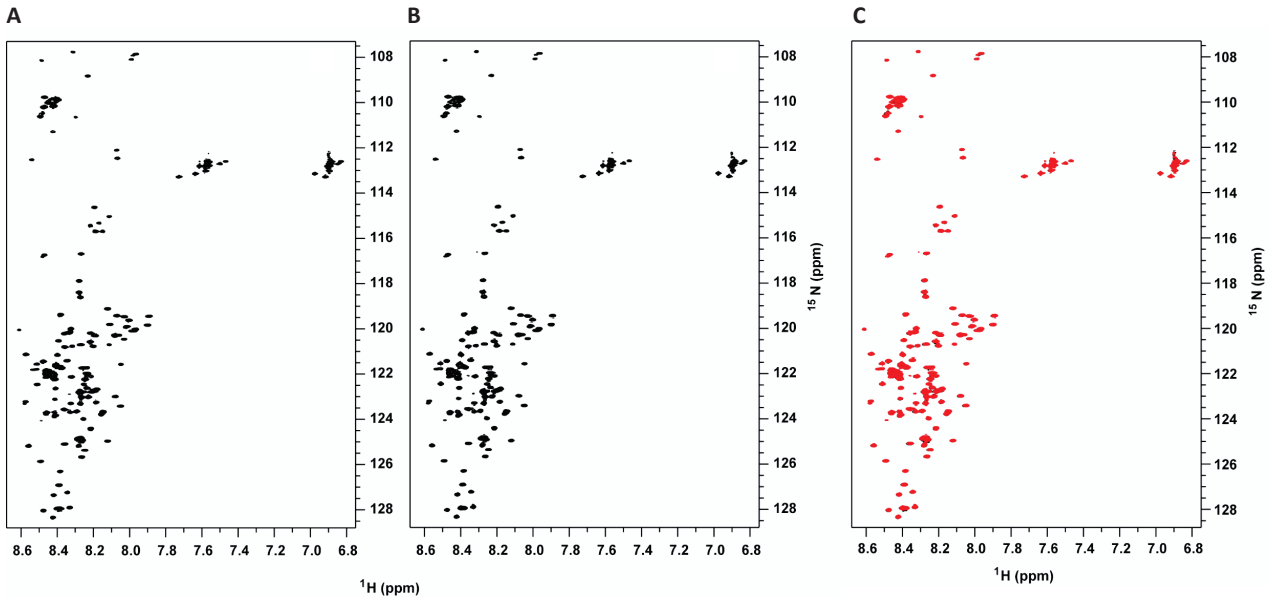

Figure S4. NMR characterisation of SynuClean-D non interaction to α-synuclein monomer. ^{1}H-^{15}N HSQC NMR spectra of ^{15}N-labeled α-Syn (70 **µ**M) in the absence (A) and in the presence (B) of SC-D (100 µM). Superposition of the spectra (C) shown in panels (A) and (B) illustrating that α-Syn exhibits identical NMR spectra in the absence (black contours) and in the presence (red contours) of SC-D.

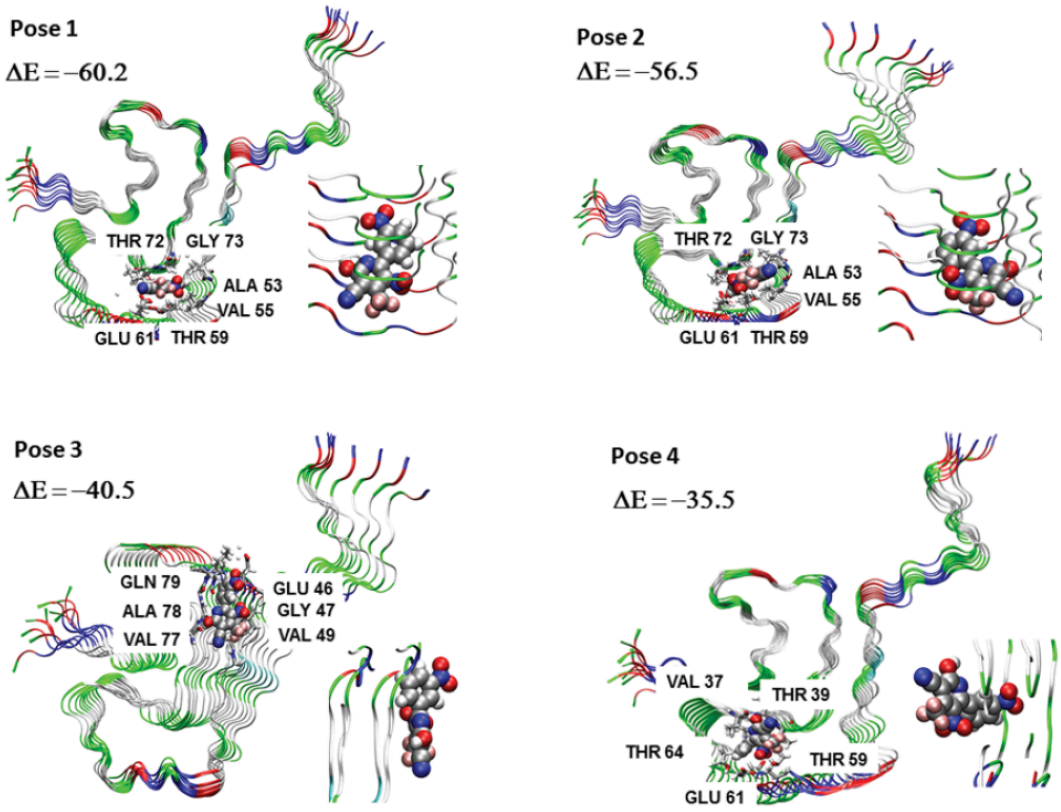

Figure S5. Binding sites prediction. Binding sites predicted by the Protein Energy Landscape Exploration (PELE) methodology. Interaction energies (DE) are expressed in kcal mol^{-1}.

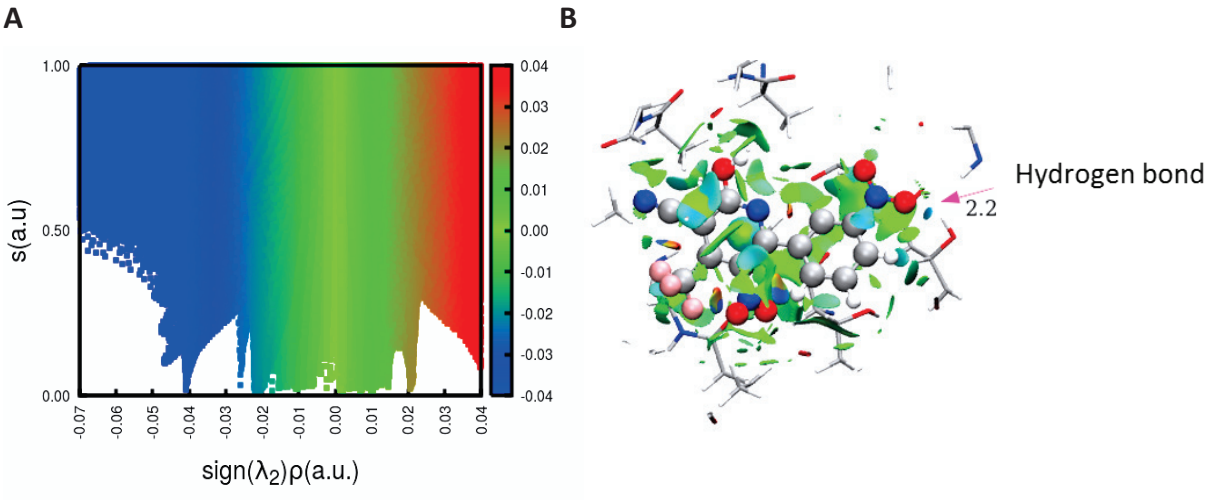

Figure S6. Characterisation of SynuClean-D-fibril interaction. Non-covalent interaction plot (A) and the representation of the non-covalent interactions involving SC-D in preferred binding pose at the PELE geometry (B). Contacts are represented in green. Distances in Å.

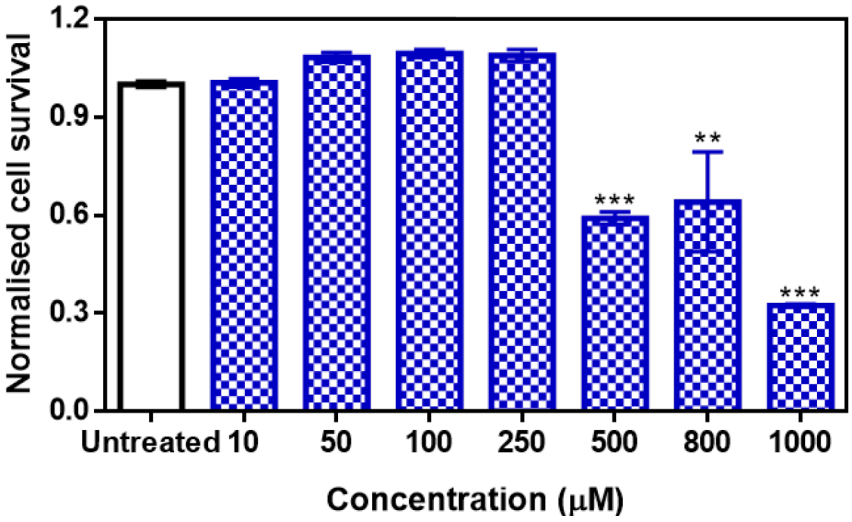

Figure S7. Toxicity of SC-D for neuroblastoma cells. Normalized SH-SY5Y cells survival in the presence of increasing concentrations of SC-D (blue) and without the compound (white).

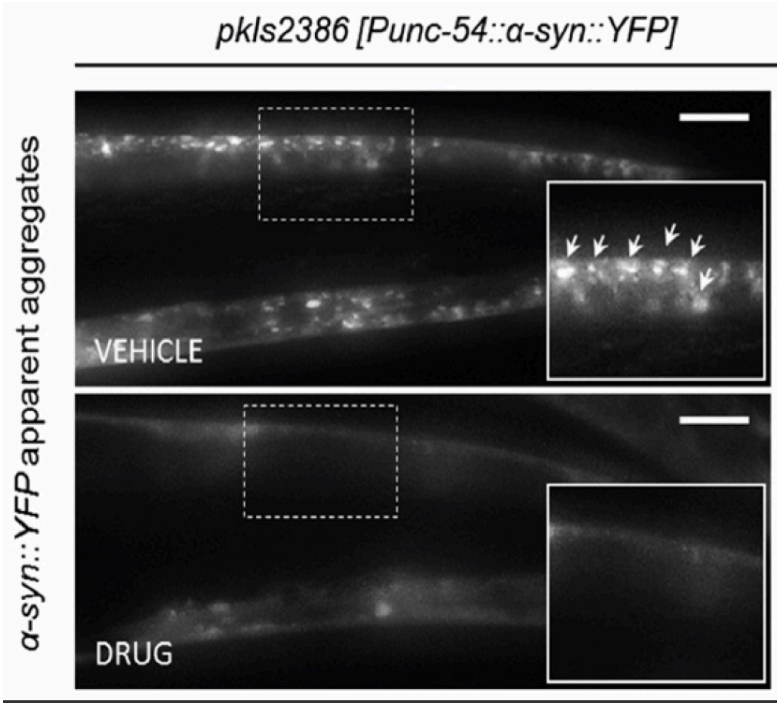

Figure S8. Inhibition effect of the compound in the formation of α-synuclein inclusions in a *C. elegans* model of PD. Selected images of α-Syn muscle aggregates obtained by epifluorescence microscopy of NL5901 worms treated without (top panel, vehicle) and with SC-D (bottom panel, drug).

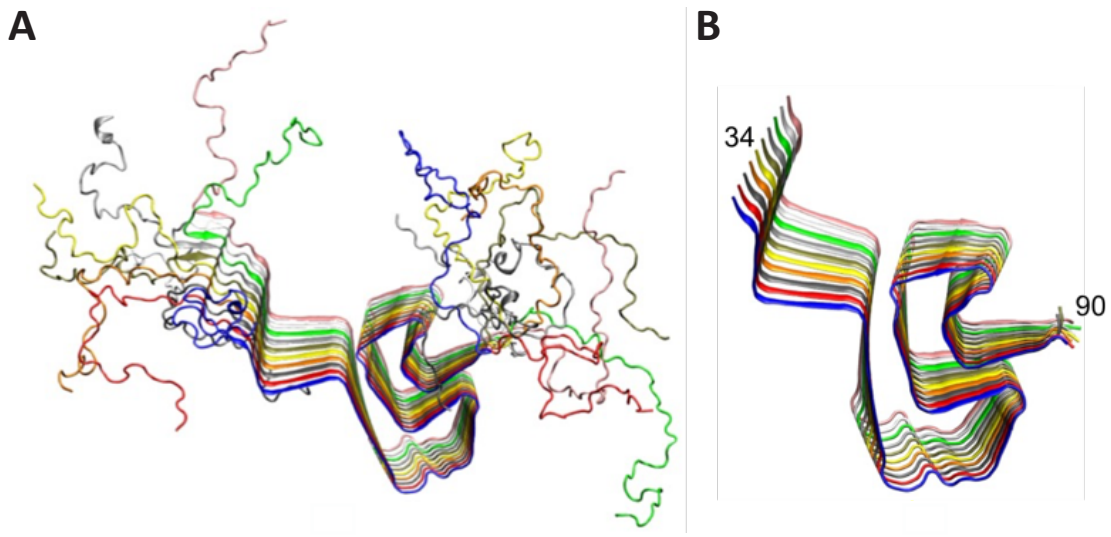

Figure S9. Aggregated structure of human α-synuclein (PDB code 2N0A). NMR full-length model of human α-Syn fibril (A). Reduced model (B), including residues 34 to 99 of PDB 2N0A employed in the binding site search and binding energy calculations.

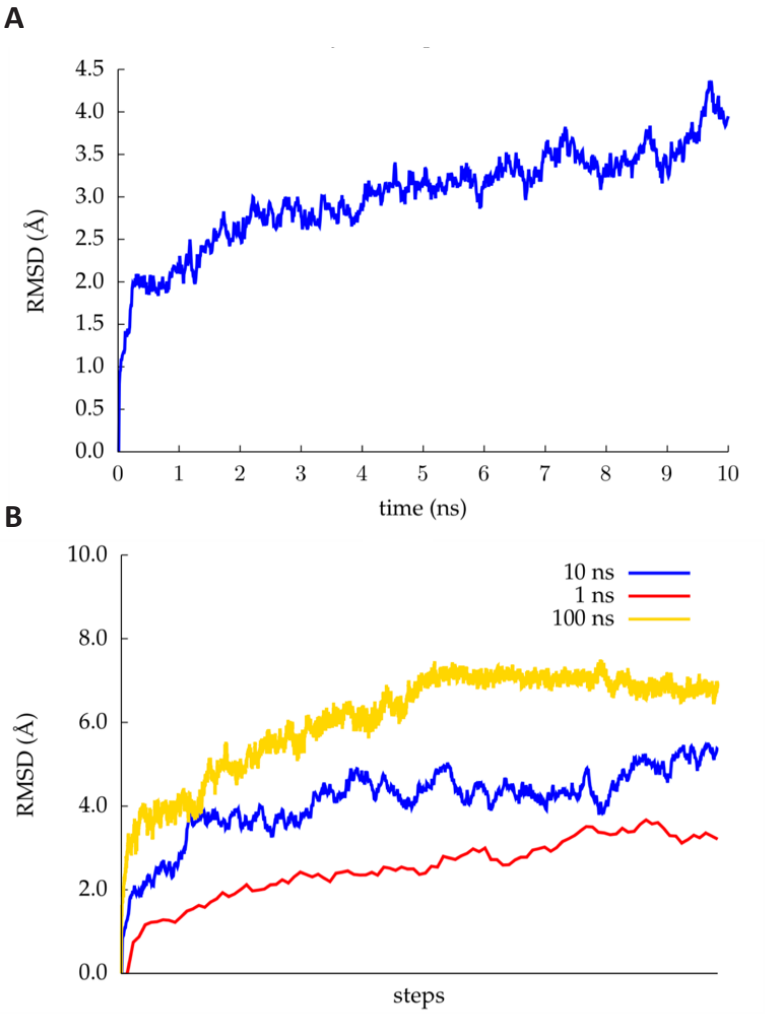

Figure S10. RMSD results of NPT molecular dynamics simulations. Backbone RMSD along 10 ns of NPT molecular dynamics simulation (A) at 300 K of the full α-synuclein fibril from PDB structure 2N0A, with RMSD computed on residues 34 to 99. Backbone RMSD computed along 1, 10 and 100 ns of NPT molecular dynamics simulations (B) of the reduced α-Syn fibril model comprising residues 34 to 99.

Table S1. Interaction energies values involved in different predicted binding sites. MM/GBSA gas phase binding energy ΔG_{gas}, van der Waals (vdW) and electrostatic contributions (E_{El}), solvation free energy (DDG_{solv}), and binding energy in solution (ΔG_{bind}) for the two internal (1 and 2) and two external (3 and 4) poses of SC-D interacting with the α-Syn fibril model. All energies are in kcal mol^{-1}. Standard deviation is showed in parentheses.

Binding pose	***1***	***2***	***3***	***4***
ΔG_{gas}	-53.7 (5.4)	-47.1 (9.5)	-40.6 (8.3)	-52.3 (16.6)
vdW	-36.2 (4.5)	-37.1 (4.7)	-25.0 (3.9)	-31.0 (5.0)
E_{El}	-17.5 (4.7)	-10.0 (10.3)	-15.6 (7.0)	-21.3 (13.3)
$D\Delta G_{solv}$	35.3 (4.6)	32.5 (8.1)	29.2 (6.8)	36.2 (12.2)
ΔG_{bind}	-18.4 (4.1)	-14.6 (3.4)	-11.4 (3.1)	-16.1 (5.7)

Movie S1. Mobility of untreated YFP::α-SYN worms, at day 7 of adulthood.

Movie S2. Mobility of YFP::α-SYN worms treated with 10 μM of SC-D, at day 7 of adulthood.

References

1. Pujols J*, et al.* (2017) High-Throughput Screening Methodology to Identify Alpha-Synuclein Aggregation Inhibitors. *Int J Mol Sci* 18(3).
2. Crespo R*, et al.* (2016) What Can the Kinetics of Amyloid Fibril Formation Tell about Off-pathway Aggregation? *J Biol Chem* 291(4):2018-2032.
3. Tuttle MD*, et al.* (2016) Solid-state NMR structure of a pathogenic fibril of full-length human alpha-synuclein. *Nat Struct Mol Biol* 23(5):409-415.
4. Madadkar-Sobhani A & Guallar V (2013) PELE web server: atomistic study of biomolecular systems at your fingertips. *Nucleic Acids Res* 41(Web Server issue):W322-328.
5. Borrelli KW, Vitalis A, Alcantara R, & Guallar V (2005) PELE: Protein Energy Landscape Exploration. A Novel Monte Carlo Based Technique. *J Chem Theory Comput* 1(6):1304-1311.
6. Onufriev A, Bashford D, & Case DA (2000) Modification of the generalized Born model suitable for macromolecules. *Journal of Physical Chemistry B* 104(15):3712-3720.
7. Jorgensen WL & Tirado-Rives J (1988) The OPLS [optimized potentials for liquid simulations] potential functions for proteins, energy minimizations for crystals of cyclic peptides and crambin. *J Am Chem Soc* 110(6):1657-1666.
8. Salomon-Ferrer R, Case DA, & Walker RC (2013) An overview of the Amber biomolecular simulation package. *Wiley Interdisciplinary Reviews-Computational Molecular Science* 3(2):198-210.
9. Genheden S & Ryde U (2015) The MM/PBSA and MM/GBSA methods to estimate ligand-binding affinities. *Expert Opinion on Drug Discovery* 10(5):449-461.
10. D.A. Case DSC TEC, III, T.A. Darden, R.E. Duke, T.J. Giese, H. Gohlke, A.W. Goetz, D. Greene, N. Homeyer, S. Izadi, A. Kovalenko, T.S. Lee, S. LeGrand, P. Li, C. Lin, J. Liu, T. Luchko, R. Luo, D. Mermelstein, K.M. Merz, G. Monard, H. Nguyen, I. Omelyan, A. Onufriev, F. Pan, R. Qi, D.R. Roe, A. Roitberg, C. Sagui, C.L. Simmerling, W.M. Botello-Smith, J. Swails, R.C. Walker, J. Wang, R.M. Wolf, X. Wu, L. Xiao, D.M. York and P.A. Kollman (2016) AMBER 16. *University of California, San Francisco*.
11. Wang J, Wolf RM, Caldwell JW, Kollman PA, & Case DA (2004) Development and testing of a general amber force field. *J Comput Chem* 25(9):1157-1174.
12. Feig M*, et al.* (2004) Performance comparison of generalized born and Poisson methods in the calculation of electrostatic solvation energies for protein structures. *J Comput Chem* 25(2):265-284.
13. Johnson ER*, et al.* (2010) Revealing noncovalent interactions. *J Am Chem Soc* 132(18):6498-6506.

14. Lazaro DF*, et al.* (2014) Systematic comparison of the effects of alpha-synuclein mutations on its oligomerization and aggregation. *PLoS Genet* 10(11):e1004741.
15. Harrington AJ, Yacoubian TA, Slone SR, Caldwell KA, & Caldwell GA (2012) Functional analysis of VPS41-mediated neuroprotection in Caenorhabditis elegans and mammalian models of Parkinson's disease. *J Neurosci* 32(6):2142-2153.
16. van Ham TJ*, et al.* (2008) C. elegans model identifies genetic modifiers of alpha-synuclein inclusion formation during aging. *PLoS Genet* 4(3):e1000027.
17. Munoz-Lobato F*, et al.* (2014) Protective role of DNJ-27/ERdj5 in Caenorhabditis elegans models of human neurodegenerative diseases. *Antioxid Redox Signal* 20(2):217-235.
18. Cao S, Gelwix CC, Caldwell KA, & Caldwell GA (2005) Torsin-mediated protection from cellular stress in the dopaminergic neurons of Caenorhabditis elegans. *J Neurosci* 25(15):3801-3812.